

Vortices and Edge Reconstruction in Small Quantal Systems at High Angular Momenta

M. Toreblad, Y. Yu and S.M. Reimann

Mathematical Physics, Lund Institute of Technology, SE-22100 Lund, Sweden

M. Koskinen and M. Manninen

**NanoScience Center, Department of Physics, FIN-40351 University of Jyväskylä, Finland*

Vortices can form when finite quantal systems are set to rotate. In the limit of small particle numbers the vortex formation in a harmonically trapped *fermion* system, with repulsively interacting particles, shows similarities to the corresponding boson system, with vortices entering the rotating cloud for increasing rotation. We show that for a larger number of fermions, $N \gtrsim 15$, the fermion vortices compete and co-exist with (Chamon-Wen) edge-reconstructed ground states, forcing some ground states, for instance the central single vortex, into the spectrum of excited states. Experimentally, the fermion system could for instance be a semiconductor heterostructure, a quantum dot, and the corresponding boson system a magneto optical trap (MOT).

PACS numbers: 71.10.-w, 71.15.-m, 03.75.Lm

I. INTRODUCTION

Macroscopically, the appearance of vortices is an everyday phenomenon. Hardly anyone has missed the swirl of water going down the drain, or the vortices forming while stirring in a cup of coffee. Correspondingly, on the microscopic level the formation of vortices and vortex lattices is known to lower the energy of a rotating quantum system. A vortex is then characterised by a singularity encircled by annular currents.

In the 50's Abrikosov predicted the existence of vortices in superconductors subject to a magnetic field¹. Almost 50 years later, in 2001, Abo-Shaeer *et al.*² found vortices forming in rotating Bose-Einstein condensates. These many-body systems consist of paired electrons and bosonic atoms, respectively. Mean-field approaches are often employed to describe the complex structures that these systems comprise. For Bose-Einstein condensates, one often applies the Gross-Pitaevskii equation. In this way, Butts and Rokhsar³ and later on Kavoulakis, Pethick and Mottelson^{4,5} found successive transitions between stable patterns of singly-quantised vortices, as the angular momentum was increased.

Surprisingly vortex solutions, as discussed above, can also be found in small fermion systems with non-paired, repulsively interacting particles at large angular momenta^{6,7}. Such systems could, for instance, be realized in quantum dots⁸ (small semiconductor islands confining a finite number of electrons) at high magnetic fields. Incredibly enough, the vortex formation by repulsively interacting fermions at high angular momenta is very similar to the bosonic case⁷: Irrespective of the system being bosonic or fermion, vortex solutions govern the ground states in the limit of large angular momenta.

Setting a cloud of fermions rotating is equivalent to applying a strong magnetic field. For an electron in a quantum dot, at a certain field strength the system spin-polarises, and forms a compact droplet where the N particles occupy neighbouring single-particle orbitals with angular momenta $m = 0, 1, 2, \dots, (N-1)$, all belonging to

the so-called lowest Landau level (LLL) with radial quantum numbers $n_r = 0$. This compact, so-called “maximum density droplet” (MDD)⁹ is the finite-size analog to integer filling factors in the bulk¹⁰. At larger fields or similarly, for higher total angular momenta, the droplet reconstructs its charge distribution. Different scenarios have been suggested (see⁸ for a review): While in the low- N limit, the formation of holes at the centre was discussed by MacDonald, Yang and Johnson^{9,11}, Chamon and Wen¹² suggested that for larger droplets, the energy could be lowered by splitting off a (homogeneous) ring of electrons. In fact, it turned out later that the formation of a charge density wave along the edge was even more favourable¹³.

In this article we re-investigate the reconstruction of the maximum density droplet (MDD) in the light of vortex patterns and the apparent analogy to the bosonic case. We show that, in agreement with the earlier findings of Yang *et al.*¹¹, reconstruction of the MDD begins from the edge rather than the dot centre if the electron number exceeds $N \approx 15$. At smaller dot sizes, however, vortices enter the MDD from the edge, in much analogy to the bosonic case⁷. The universality between fermion and boson systems discussed by Toreblad *et al.*⁷ holds up to $N \approx 15$. For higher N , not all vortex solutions appear as ground states. Instead edge reconstruction takes over at the onset of the MDD break-up. In the limit of very large angular momenta, vortices can co-exist with the usual (Chamon-Wen) edge-reconstructed ground states.

II. MANY-BODY ASPECTS OF THE HARMONIC OSCILLATOR

The Hamiltonian H_Ω , which we investigate, is of two-dimensional nature and describes an interacting finite many-body system under rotation (or, equivalently, subject to a magnetic field, see appendix) which is confined

by a harmonic oscillator potential:

$$\begin{aligned} H_\Omega &= \sum_{i=1}^N \left(\frac{\mathbf{p}_i^2}{2m} + \frac{1}{2}m\omega_0^2 \mathbf{r}_i^2 \right) + \sum_{i < j}^N v(\mathbf{r}_i - \mathbf{r}_j) - \Omega L_z = \\ &= H - \Omega L_z. \end{aligned} \quad (1)$$

Here m is the particle mass and ω_0 the confining frequency of the oscillator. This Hamiltonian has, in fact, become the standard choice to model finite quantal systems – it equally well describes the physics of electrons trapped in a quantum dot⁸, as bosonic or fermion atoms in a magneto-optical trap¹⁴. The two-dimensionality originates in the quantum dot from the semiconductor heterostructure. In the atom trap, it can be designed by the experimental set-up. In addition, strong rotational motion lowers the effective confinement perpendicular to the axis of rotation. This leads to a ground state with only the lowest energy level occupied along the z -direction^{15,16}.

The operator $-\Omega L_z$ adds rotation at an angular frequency Ω . Since the total angular momentum, L , is a good quantum number to H_Ω , it effectively subtracts a term ΩL from the energy of the Hamiltonian H . As a result a larger Ω will create a ground state with higher total angular momentum. Instead of seeking solutions at varying Ω , we follow the tradition in nuclear physics and solve H for a given L to obtain the total energy, E_L , and the many-body state $|\Psi_{F,B}(L)\rangle$. Note, that the lowest state for a fixed L is not necessarily the ground state of H_Ω . To find that state, we still need to subtract ΩL .

As is usually done for these systems, the interaction between the electrons in a quantum dot is modelled by the ordinary Coulomb repulsion:

$$v(\mathbf{r}_i - \mathbf{r}_j) = \frac{e^2}{4\pi\epsilon\epsilon_0|\mathbf{r}_i - \mathbf{r}_j|}.$$

For trapped, dilute atomic gases it is well known¹⁴ that the interaction between the particles are more realistically described by a zero-range potential of the form $a\delta(\mathbf{r}_i - \mathbf{r}_j)$, where a is the scattering length¹⁴. However, we have recently shown that the dominating features in the boson many-body spectra are to a large extent independent of the two-body interaction⁷, and very similar results were obtained both for short-range and Coulomb two-body forces in the lowest Landau level. For ease of comparison with the electron system under consideration, we thus restrict this study to the usual Coulomb interaction, *both* in the fermion *and* boson case. To simplify the comparison further, only *one spin state* will be considered: Spin-polarised fermions and bosons with zero spin.

In second quantisation, here for fermions, we write

$$H = \sum_{i,j=1}^{\infty} \langle i|h|j\rangle \hat{c}_i^\dagger \hat{c}_j + \frac{1}{2} \sum_{i,j,k,l=1}^{\infty} \langle ij|v_{coul}|kl\rangle \hat{c}_i^\dagger \hat{c}_j^\dagger \hat{c}_l \hat{c}_k, \quad (2)$$

where h stands for the single-particle part of the Hamiltonian in Eq. (1), $\{|i\rangle\}_{i=1}^{\infty}$ is the harmonic oscillator basis

and \hat{c}_i^\dagger and \hat{c}_i are the corresponding creation and annihilation operators. One can now simply construct the full Hamiltonian matrix and diagonalise it to obtain the energies and corresponding many-particle states. The many-particle solution $|\Psi_F\rangle$ for fermions is then given by an expansion in Slater determinants $|\psi_i\rangle$,

$$|\Psi_F\rangle = \sum_i c_i |\psi_i\rangle. \quad (3)$$

For the bosonic, symmetric solution $|\Psi_B\rangle$, Eq. 2 is similar, with the fermion operators exchanged for the corresponding boson operators \hat{b}_i^\dagger and \hat{b}_i .

This so-called “exact” diagonalisation is the brute-force method of many-body quantum mechanics. However, to name the method “exact” is misleading. A full Hamiltonian matrix would be infinitely large, which of course would be impossible to handle. A further complication is the fact that the size of the Hamiltonian matrix rapidly increases, making calculations for more than about six particles extremely time-consuming. In view of the structure of the single particle levels for high magnetic fields⁸, we thus restrict the single particle states to the above mentioned lowest Landau level (LLL). Physically this means that we ignore high energy excitations which would mix the lowest and higher Landau levels. For both bosons and fermions this is a common restriction, which is justifiable for dilute quantum gases at very high angular momenta, or at very high magnetic fields. It allows us to extend the studies to systems with up to 25 particles.

III. APPEARANCE OF VORTICES IN BOSONIC AND FERMIONIC SYSTEMS

In weakly interacting bosonic systems, which are set rotating, successive transitions between stable vortex states have been found³ for increasing angular momentum. In particular, in a rotating and weakly interacting bosonic system with a short-range interaction, solutions of the Gross-Pitaevskii equation have revealed^{4,5} a central one-vortex solution for the ratio of angular momentum to particle number being equal to one, $l = L_{1V}^B/N = 1$, a two-vortex solution at $l = L_{2V}^B/N \approx 1.75$ and a three-vortex state at $l = L_{3V}^B/N \approx 2.1$ (in atomic units).

Assuming similar vortex formation in the (unpaired) fermion system the vortex angular momenta are shifted by $N(N-1)/2$ as compared to the boson system. This shift corresponds to the many-body configuration of the MDD, which is the fermion equivalent to the boson many-particle ground state. An intuitive explanation is given by the configurations of the Fock states in the LLL, i.e. $|n_0 n_1 n_2 \dots n_m \dots\rangle$, where n_m is the number of particles in the single-particle state with angular momentum m . In the non-rotating ground state in the bosonic case all N spin-less particles are occupying the lowest single-particle orbital, the Fock state being of the form $|N0000 \dots 000\rangle$. For spin-polarised fermions, the Pauli principle demands single occupancies up to the Fermi

surface, and the Fock state of the MDD is a single Slater determinant of the form $|111\cdots 111000\cdots 000\rangle$. As the angular momentum of the MDD equals $N(N-1)/2$, a central single vortex in the fermion case should appear at $l = (L_{1V}^F - L_{MDD})/N = 1$, a two-vortex solution at $l = (L_{2V}^F - L_{MDD})/N \approx 1.75$, and a three-vortex solution correspondingly at $l = (L_{3V}^F - L_{MDD})/N \approx 2.1$.

IV. COMPARISON BETWEEN ROTATING FERMION AND BOSON SYSTEM

Let us now investigate the rotating fermion system as compared to the rotating boson system. In the lowest Landau level, at fixed angular momentum L the total energy is given by

$$E_L = \hbar\omega_0(L+N) + \langle \Psi_{F,B}(L) | v | \Psi_{F,B}(L) \rangle,$$

where the first term originates from the kinetic energy and the confining potential, and the second term from the interaction energy. An increase in $\hbar\omega_0(L+N)$ indicates a centre of mass excitation, whereas variations in $\langle \Psi_{F,B}(L) | v | \Psi_{F,B}(L) \rangle$ imply changes in the interaction energy, which affects the configuration.

Computationally, there now exist two more simplifying circumstances: (1) The kinetic energy and the confining potential constitute a diagonal term to the total energy. It is therefore sufficient to diagonalise only $\langle \Psi_{F,B}(L) | v | \Psi_{F,B}(L) \rangle$ and add the term $\hbar\omega_0(L+N)$ at the end to obtain the total energy. The outcome will be the same as including the diagonal terms in the diagonalisation. (2) The interaction is independent of confining frequency, ω_0 , since

$$\langle \Psi_{F,B}(L) | v | \Psi_{F,B}(L) \rangle |_{\omega_0=\omega} = \sqrt{\omega} \langle \Psi_{F,B}(L) | v | \Psi_{F,B}(L) \rangle |_{\omega_0=1}.$$

This can easily be verified by writing the expression with second quantisation and comparing the integrals for $\omega_0 = \omega$ and $\omega_0 = 1$ a.u. The results presented are thus independent of confining frequency and it is only necessary to study $\omega_0 = 1$ a.u. as long as only the lowest Landau level is considered.

The interaction energy versus angular momentum is displayed in Fig. 1 for fermions (a) and bosons (b). Following the tradition in nuclear physics, the dashed line connecting the lowest states at fixed L is called the “yrast” line¹⁷, and the spectrum of H the yrast spectrum. The interaction energy is plotted as a function of the above defined unit less variable l , which in a boson system corresponds to $l = L/N$ and in a fermion system to $l = (L - L_{MDD})/N$. By this construction we simplify the comparison between boson and fermion systems, and it also becomes easier to compare systems of differing particle number. Note that $l = 0$ in the fermion system corresponds to the MDD. In the boson system, it describes the $L = 0$ ground state.

Not surprisingly, both in the boson and fermion spectra (as shown for $N = 12$ in Figure 1) the interaction energy decreases with increasing l : A larger l -value implies a higher rotation, which pushes the particles further

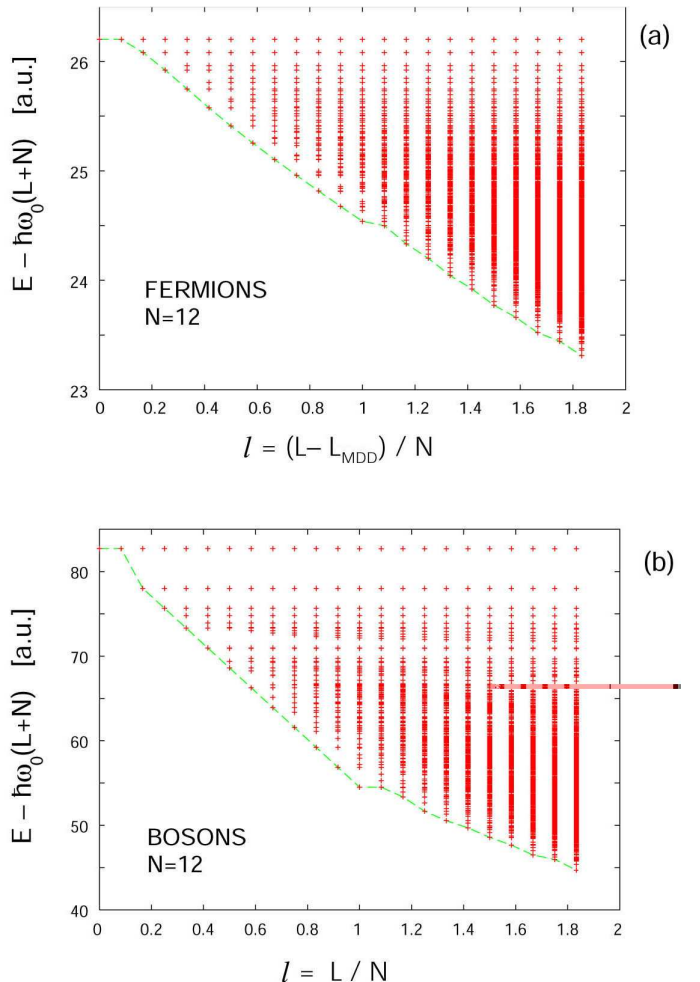


FIG. 1: Interaction energy versus angular momentum for a system of 12 harmonically trapped, spin-less particles interacting with a Coulomb repulsion, in (a) for fermions, and in (b) for bosons. The dashed line is the so-called yrast line, connecting the lowest-energy states.

apart. However, the spectra reveal other striking similarities. Recalling the fact that, due to the Pauli principle, the fermion total angular momenta are displaced with respect to the boson systems by the angular momentum of the MDD, we realize that the spectra for fermions and bosons are very similar. The yrast line in both cases shows a pronounced kink at $l = 1$, and fainter kinks are observed at $l = 1.67$ and at $l = 1.83$ (not shown in Fig. 1). For the boson system we know these particular l -values to be related to the formation of vortices. According to the previously discussed results of the Gross-Pitaevskii equations a one-vortex solution corresponds to exactly $l = 1$, and a two-vortex solution to $l \approx 1.75$. What happens in the fermion system?

Before studying the many-particle states in more detail, it is interesting to explore which l -values correspond to ground states in the rotating system. In Figure 2 the ground states for increasing Ω have been found by subtracting ΩL from E_L . Intriguingly, most of the l -values

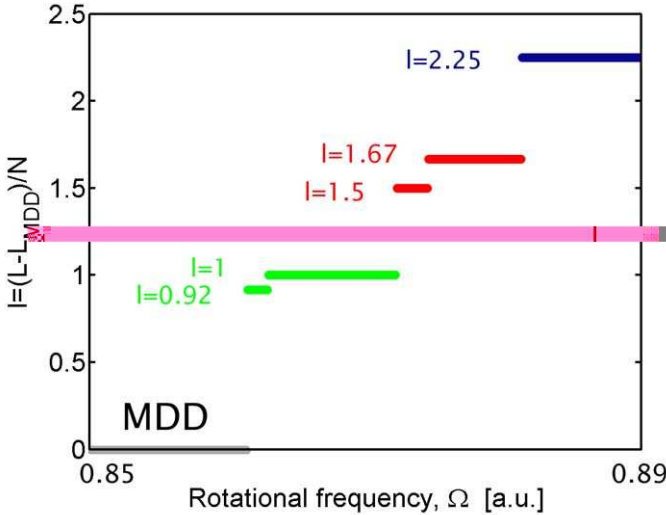


FIG. 2: By taking $E_L - \Omega L$ for increasing total angular momentum the ground state values of $l = (L - L^{MDD})/N$ are found in a rotating system of 12 fermions as a function of the rotational frequency, Ω . For increasing rotation the ground state is shifted from the MDD ($l = 0$) to higher total angular momentum. In the figure successive transitions to states $l \approx 1$, $l \approx 1.6$ and to $l = 2.25$ occur. For computational reasons higher l -values have not considered.

corresponding to kinks of the yrast line, including intermediate values $l = 0.92$ and 1.5 , now reappear. (Note that to increase Ω above 1 a.u. has no physical meaning. If the rotational frequency exceeds the confining frequency the effective confinement disappears, see appendix.)

To extract information from the many-particle wavefunctions, one must process the data in some way. Two informative quantities are the occupancies, P_m , of the single particle states, which illustrates to what extent each single particle state (in the LLL) is present in the many-body configuration, and the radial particle densities,

$$\rho(\mathbf{r}) = \langle \Psi_{F,B}(L) | \sum_{i=1}^N \delta(\mathbf{r} - \mathbf{r}_i) | \Psi_{F,B}(L) \rangle,$$

where $\mathbf{r} = (r, 0)$ in polar coordinates. The occupancies describe which single particle states dominate. If, for instance, $P_{m=0}$ has a magnitude close to zero the radial density will be very small at $r = 0$, since the single particle state (in the LLL) with $m = 0$ has its maximum at $r = 0$. Similarly a minimum at $P_{m=1}$ implies a slightly off-centred minimum in the radial density. Hence, a central single vortex should appear as a minimum for $m = 0$ in the occupancy and at $r = 0$ in the radial density, and a two-vortex state as an off-centred minimum both in the occupancy and in the radial density. In Figure 3 the occupancies are plotted for the ground state values $l = 0.92, 1, 1.5, 1.67$ and 2.25 , and the excited state $l = 1.83$. The insets show the radial densities. The last state has been included for completeness. If we compare with the ground states in the bosonic system, these are

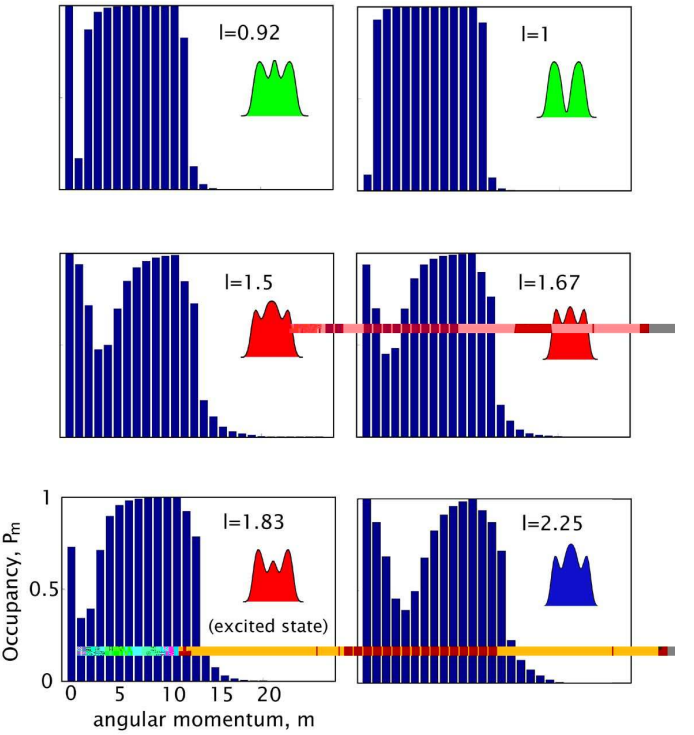


FIG. 3: The occupancies of the single particle states for a system of $N = 12$ fermions. The values $l = 0.92, 1, 1.5, 1.67$ and 2.25 correspond to the ground state values in a system rotating at an increasing frequency. The excited state $l = 1.83$ has been included for completeness. The insets show the radial densities from $r = -6a_B^*$ to $r = 6a_B^*$ for each l -value.

$l = 1, 1.67, 1.83$, and 2.25 . Even if the state $l = 1.83$ in the fermion system is not a ground state in the rotating system, it is the lowest-energy state at that particular l in the yrast spectrum. In the boson case we know that a central single vortex appears at $l = 1$ and a two-vortex solution is found at $l \approx 1.75$. As expected, in the fermion system, the central single vortex is clearly visible at $l = 1$. The two-vortex state, however, is more difficult to identify. In contrast to mean field methods, for an exact calculation with good angular momentum the particle density has circular symmetry and thus does not display the internal structure directly. The vortices are averaged over the entire circle and only show as two dips in the radial densities. The ground state with $l = 1.67$ and the excited state with $l = 1.83$ showing two minima in the radial density thus constitute likely candidates for a two-vortex state.

Another implication of many-vortex solutions in the exact result can be found in the occupancies, which display some interesting systematics. To understand these systematics better we chose to study only the structure of the Fock state with the largest magnitude in the expansion of $|\Psi_F(L)\rangle$ (see Eq. 3).

In Table I the dominating configurations and their amplitudes are shown for ground state l -values and the excited state $l = 1.83$ in the case of $N = 12$. For $l = 0.92$ a single

l	$ c_{max} ^2$	Many-body configuration
0.92	0.83	101111111111000
1.00	0.92	011111111111000
1.50	0.40	1110011111111100
1.67	0.44	1100111111111100
1.83*	0.55	1001111111111100
2.25	0.28	1110011111111100

TABLE I: The dominating many-particle configurations for $N = 12$ for the ground state l -values. Note the single, respectively double, hole for $l = 1$ and $l = 1.83$, which are the expected central single and double vortex states. ($l = 1.83$ is an excited state, as marked by a star).

hole has entered the MDD. This corresponds to the minimum shown in the occupancy in Figure 3. At $l = 1$ it has reached the centre of the cloud and the single hole state has become very dominant in the many-body configuration (consider its magnitude). Correspondingly, the radial density shows a clear central single vortex. At $l = 1.5$ a double hole starts to enter the MDD. It moves further towards the centre at $l = 1.67$ and in the excited state $l = 1.83$ it has reached the position, where its amplitude is the largest. This configuration seems to be a double hole close to the centre of the fermion cloud. Could it be a two-vortex state? At $l = 2.25$ a triple hole begins to enter the MDD.

As compared to mean-field approaches, these “exact” solutions retain the circular symmetry of the Hamiltonian. In order to reveal the internal structure of the many-body wave function, methods such as calculating the pair correlation, looking at a slightly asymmetric confinement potential¹⁸ or adding a small perturbation⁷ have to be used. Especially for small N , the above methods have shown useful: When, for example, studying pair correlations, fixing one of the very few particles was found to cause too much disturbance in the fermion many-particle configuration to get a meaningful result.

V. PAIR CORRELATIONS

The pair correlation fixes one particle at a point \mathbf{r}_A and calculates the density of the remaining $N - 1$ particles.

$$P(\mathbf{r}, \mathbf{r}_A) = \frac{\langle \Psi_{F,B}(L) | \sum_{i \neq j} \delta(\mathbf{r} - \mathbf{r}_i) \delta(\mathbf{r}_A - \mathbf{r}_j) | \Psi_{F,B}(L) \rangle}{(N-1) \langle \Psi_{F,B}(L) | \sum_j \delta(\mathbf{r}_A - \mathbf{r}_j) | \Psi_{F,B}(L) \rangle}.$$

For large bosonic systems this shows the vortices clearly, see for instance Kavoulakis *et al*⁵.

However, in the limit of small N , particularly in the fermion case, the removal of one particle effects the density of the remaining particles significantly, and the result can be ambiguous: Due to the Pauli principle the point, \mathbf{r}_A , at which one fermion has been fixed, will be avoided by the other fermions. A minimum will arise in the pair correlation at this point called the exchange hole.

This makes the detection of vortices in the pair correlations very tedious. Particularly in the limit of small N , a small displacement of the reference point \mathbf{r}_A alters the pair correlations considerably.

To come about this difficulty, two schemes have previously been suggested: (*i*) adding a perturbation to the harmonic potential⁷, and (*ii*) breaking the rotational symmetry, for instance by deforming the confinement¹⁸. However, it appears that $N = 12$ is sufficiently large to study the pair correlations. The pair correlations for $N = 12$ have been plotted in Figure 4 (fermions) and Figure 5 (bosons) for the ground state values of l in both the fermion and bosonic case. For completeness, the excited state $l = 1.83$ has also been added in the fermion case. Apart from this state and the two intermediate states $l = 0.92$ and 1.5 , there is an exact correspondence in the ground state l -values of the fermion and boson systems. With respect to angular momentum, this corresponds to the shift of the angular momentum L_{MDD} of the maximum density droplet in the fermion system. Studying the pair correlations for these l -values, the entering vortex in the rotating system can clearly be seen, first changing to a central single vortex state at $l = 1$, and then to a double at $l = 1.83$. This (excited) state is the same two-vortex solution as in the bosonic case, appearing at similar l . The solution at $l = 2.25$ shows a third vortex entering, as expected from the occupancies. Note how the Pauli principle affects the fermion pair correlations by introducing the exchange hole (as marked by a black dot in Fig. 4). Naturally, this exchange hole is not present in the corresponding boson pair correlations. These are plotted in Figure 5 for comparison. We note that although the pair correlations in general are a bit ambiguous and the results depend strongly on the choice of the reference point, this method was earlier shown⁵ to yield a similar picture of vortex entry into the rotating cloud as the Gross-Pitaevskii approach⁴.

Compared to the mean-field picture the minima will not equal zero due to the zero-point oscillations present in the exact diagonalisation results.

VI. EDGE RECONSTRUCTION

For particle numbers larger than approximately 15 the central single vortex disappears from the lowest state at $l = 1$ and moves up into the spectrum of excited states. It appears that, in the fermion system, the vortex configuration is not as favourable anymore¹¹.

In figure 6 the yrast spectrum for $N = 20$ fermions is displayed for increasing values of l . A second order polynomial, $al^2 + bl + c$, has been subtracted from the interaction energy in order to display the structure of the spectrum in greater detail. In fact, below $l = 0.9$, the entering vortex state dominates as it did for smaller particle numbers. However, at $l = 0.9$, there exists a level crossing in the yrast spectrum. The state with the entering vortex becomes an excited state, which corresponds to the central one-vortex configuration at $l = 1$, while a

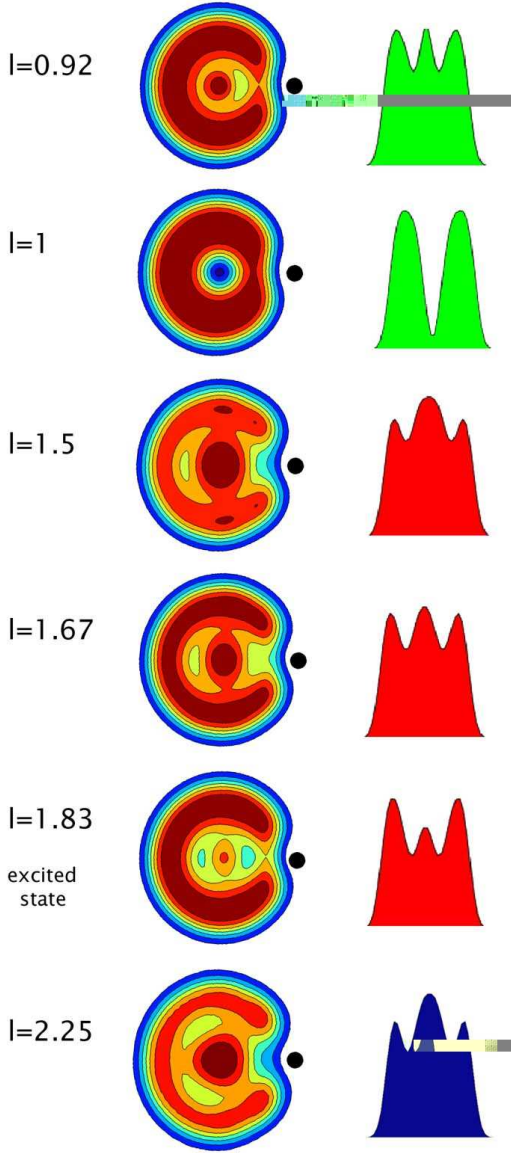


FIG. 4: Contours of the pair correlation (left panel; the black dots mark the exchange hole and the scale goes from minimum at dark blue to maximum at dark red) and radial density profiles (right panel) for $N = 12$ at $l = 0.92, 1, 1.5, 1.67, 1.83$ and 2.25 . The vortices seem to enter the cloud from the outer regions, and then move towards the centre. At $l = 1$ a central single vortex can be seen and at $l = 1.83$ a two-vortex solution exists.

state with a distinct edge becomes most prominent above $l = 0.9$. Similarly, the l -values at which the actual ground states occur in the rotating spectrum, are altered. The central one-vortex, respectively the entering two-vortex at $l = 1$ and $l \approx 1.7$, which we saw for 12 fermions, no longer appear as ground states. Instead, configurations around $l = 0.6$, $l = 1.2$ and $l = 1.8$ have become more favourable in energy. All three constitute states with a clear edge, and in particular $l = 0.6$ and $l = 1.2$ are interesting since their edges consist of localised fermions,

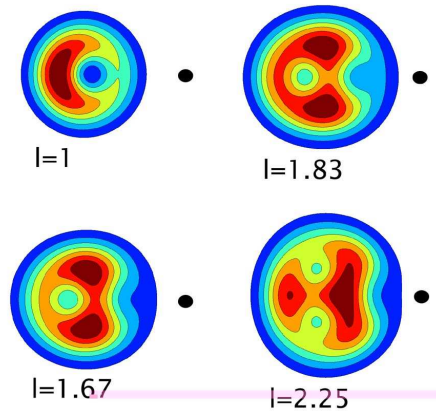


FIG. 5: Contours of the pair correlation for $N = 12$ bosons, plotted as in Fig. 4. The reference point is marked with a black dot.

so-called Chamon-Wen edges (see Figure 9). This is in contrast to the rotating boson system which is known^{3,4} to have a central one-vortex ground state at $l = 1$.

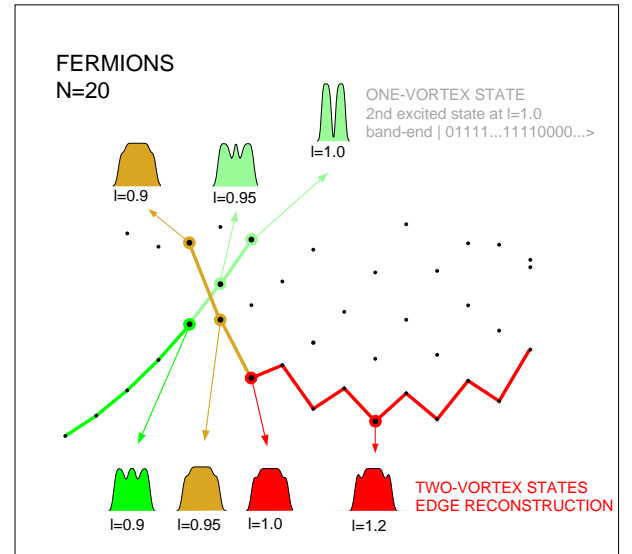


FIG. 6: Low-lying many-body states as a function of l for $N = 20$ fermions. A polynomial $al^2 + bl + c$ has been subtracted from the exact many-body energies to display the structure of the spectrum in greater detail. Just below the central unit vortex, a level crossing occurs: The single vortex state (green line) moves upwards in energy, and is replaced by an edge reconstructed ground state.

A Chamon-Wen edge becomes favourable when a higher rotation (or magnetic field) effectively decreases the radius of the single particle states as compared to the confining trap. For a rotating system at high angular momentum this would imply an increase in density relative to the confinement with increasing rotational motion, hence effectively compressing the system. The repulsive Coulomb interaction strongly inhibits this, and the maximum density droplet in effect redistributes its

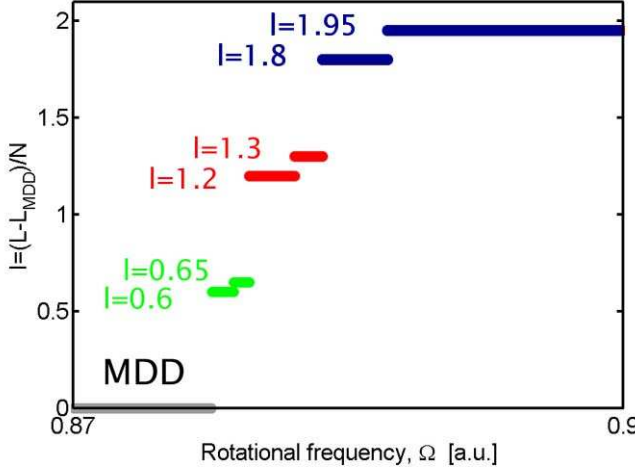


FIG. 7: Ground state l -values for increasing rotation (Ω) no longer contains the central single and double vortex states in the 20 fermion system. Instead edge reconstructed states, like $l = 0.6$ and $l = 1.2$ become dominating.

particles from lower to higher single particle momentum, leaving some states with $m < N - 1$ unoccupied, giving a ground state with $L > N(N - 1)/2$ ¹³. Figure 8 shows the occupancies and radial densities of some of the lowest energy states along the yrast line for increasing l . Both the occupancies and the radial densities imply a Chamon-Wen edge, i.e. that there exists an edge of redistributed fermions and an inner dense MDD droplet. Also visible is the entering single vortex configuration at $l = 0.9$ which becomes the second excited state in the yrast spectrum at $l = 1$ ($i = 3$). This is the central one-vortex state.

Studying also the pair correlations for $N = 20$ pictured in Figure 9 for $l = 0.6$ respectively $l = 1.2$, the edge of localised fermions is clearly visible. These pair correlations compare well with the results by Reimann *et al.*¹³, showing electron localisation along the Chamon-Wen edge within mean field current spin density functional theory (CSDFT). Note that in the exact result the localisation becomes less pronounced due to the zero point oscillations. At the first glance one might draw the conclusion that the central single vortex disappears from the lowest energy at $l = 1$ since we have increased the number of fermions in the trap. This suggests a higher particle density, which does not allow for a central minimum, the single vortex. However, the interaction energy only scales with a factor depending on ω_0 (see Sec. II). Hence, our results show that the central single vortex state will no longer be favourable irrespective of confinement frequency.

Solutions where vortices enter at the edge of the droplet, can co-exist with edge reconstructed configurations. The entering second vortex, as well as the (now off-centred) first vortex appear as two clear minima. Consider the pair correlation for $l = 1.2$ in Figure 9. A more pronounced entering two-vortex state shows in the pair correlation of $l = 1.5$ along the yrast line, also in Figure 9. This agrees well with the double hole in the occupancy of Figure 8 for the same state. The entering second vor-

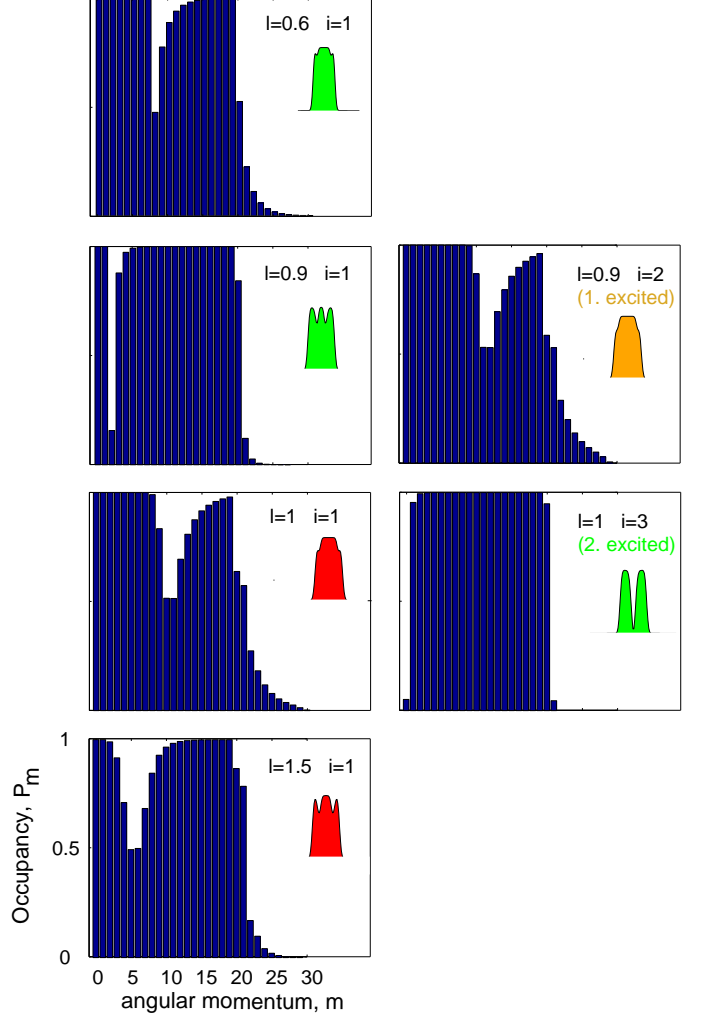


FIG. 8: Occupancies of the single particle states for a system of $N = 20$ fermions, shown for the lowest states for increasing l . Corresponding radial densities from $r = -7a_B^*$ to $r = 7a_B^*$ are shown in the insets. The central single vortex state has now disappeared from the lowest state ($i = 1$) and has become the 2nd excited state ($i = 3$) at $l = 1$.

tex can also be seen in the energy spectrum in Fig. 6 as oscillations with a period of $\Delta l = 0.1$. As explained earlier, by subtracting a second order polynomial, the oscillations in the yrast spectrum are enhanced. In Manninen *et al.*¹⁹ this was discussed in greater detail. It was found that the oscillations change period at higher l , first to become three-fold and then to become four-fold. In Figure 10 we compare the oscillation periods with holes in the Fock states, by studying the dominating configurations for increasing l . For simplicity, the lowest energy at each l -value ($E_L(i = 1)$) have been subtracted, i.e. we study the excitation spectrum. The (red) circles describe the entering vortex state, $|11 \cdots 11011 \cdots 10 \cdots \rangle$, which is seen to become the second excited state in the yrast spectrum at $l = 1$. Earlier, this was found to be the central single vortex configuration. The (green) triangles are then seen to move downwards in the spectrum

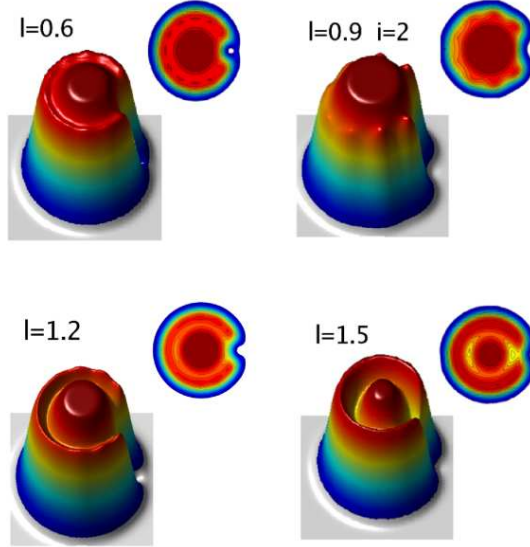


FIG. 9: Pair correlations for $N=20$ fermions for some values of l along the yrast line. In addition, $l = 0.6$ and $l = 1.2$ are ground states in the rotating system. Especially note the clear Chamon-Wen edge of the $l = 0.6$ state, which can be compared to the CSDFT result in Reimann *et al.*¹³ with $l = 0.75$.

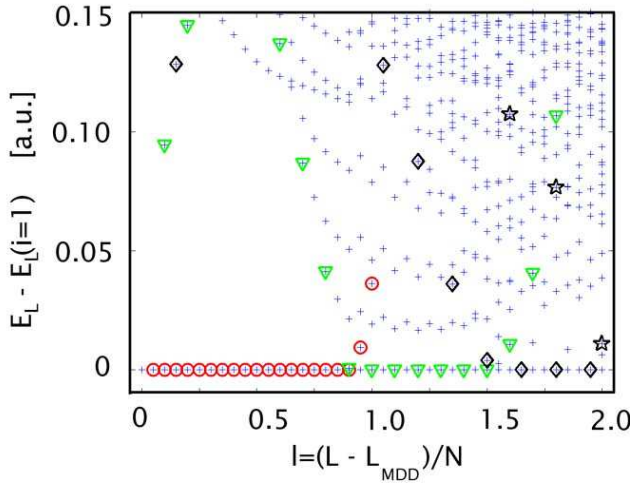


FIG. 10: Yrast spectrum for $N = 20$, with the lowest energy at fixed l ($E_L(i = 1)$) subtracted. The (red) circles mark a single zero entering the Fock state of the MDD, the (green) triangles a double hole, for example $|11 \dots 11100111 \dots 11000 \dots\rangle$ and (black) diamonds a triple hole.

for increasing l . These are the entering double vortex states, $|11 \dots 110011 \dots 10 \dots\rangle$, appearing in the energy

spectrum as oscillations with period $\Delta l = 0.1$. Moving the double hole (00) one step to the left implies an increase in total angular momentum of two. The entering double vortex, thus, only appears at every second L (in the Figure $\Delta l = 0.1$), corresponding to the double oscillations. Similarly, the entering triple vortex, (black) diamonds, with Fock state $|11 \dots 1100011 \dots 10 \dots\rangle$, can only occur at every third L , corresponding to a three-fold oscillation period. This is in exact agreement with Manninen *et al.*¹⁹.

VII. SUMMARY AND CONCLUSIONS

To conclude, the results presented have shown that there indeed exists some universal features between rotating systems of bosons and (unpaired) fermions. All calculations have been performed using the method of exact diagonalisation, and the wavefunction data have been evaluated with the aid of occupancies and pair correlations. Especially, the tendency of these systems to form vortices at similar angular momenta have been explored. However, for larger particle numbers than approximately 15 the central single vortex state becomes an excited state and the ground state, instead, lowers its energy by reconstructing to form an edge of localised fermions. This is in agreement with earlier mean-field computations, see for instance Reimann *et al.*¹³.

Acknowledgements

We thank B. Mottelson, D. Pfannkuche, H. Saarikoski, E. Räsänen, A. Harju and M. Puska for rewarding discussions. Financial support from the Swedish Foundation for Strategic Research and the Swedish Research Council is gratefully acknowledged.

APPENDIX: ANALOGY BETWEEN ROTATION AND MAGNETIC FIELD

Consider the Hamiltonian of the rotating system, Eq. (1), in Sect. II. Re-writing H_Ω , we show that it equally well corresponds to a harmonic oscillator subject to an effective magnetic field of strength $B = \nabla \times (m\Omega \hat{z} \times \vec{r}/e) = (2m\Omega/e)\hat{z}$ and with a confinement frequency $(\omega_0^2 - \Omega^2)$ ¹⁶:

$$H_\Omega = \sum_{i=1}^N \left(\frac{(\mathbf{p}_i - m\Omega \hat{z} \times \mathbf{r}_i)^2}{2m} + \frac{1}{2}m(\omega_0^2 - \Omega^2)\mathbf{r}_i^2 \right) + \sum_{i < j}^N \frac{e^2}{4\pi\epsilon_0|\mathbf{r}_i - \mathbf{r}_j|}$$

As a consequence, the rotation effectively lowers the confinement in x-y-direction to $(\omega_0^2 - \Omega^2)$.

¹ A. A. Abrikosov, Zh. Eksperim. i Teor. Fiz. **32**, 1442 (1957); [English transl.: Soviet Phys. JETP 5, 1174

(1957)].

² J.R. Abo-Shaer, C. Raman, J.M. Vogels, W. Ketterle, *Science* **292**, 476 (2001).

³ D.A. Butts, and D.S. Rokhsar, *Nature* **397**, 327 (1999)

⁴ G. M. Kavoulakis, B. Mottelson and C. J. Pethick, *Phys. Rev. A* **62**, 063605 (2000).

⁵ G. M. Kavoulakis, S. M. Reimann and B. Mottelson, *Phys. Rev. Lett.* **89**, 079403 (2002).

⁶ H. Saarikoski, A. Harju, M.J. Puska, and R.M. Nieminen, *Phys. Rev. Lett.* **93**, 116802 (2004)

⁷ M. Toreblad, M. Borgh, M. Koskinen, M. Manninen and S.M. Reimann, *Phys. Rev. Lett.* **93**, 090407 (2004).

⁸ S.M. Reimann and M. Manninen, *Rev. Mod. Phys.* **74**, 1283 (2002).

⁹ A.H. MacDonald, S.R.E. Yang, and M.D. Johnson, *Aust. J. Phys.* **46**, 345 (1993).

¹⁰ E. Prange, and S.M. Girvin, Eds., *The Quantum Hall Effect*. (Springer, New York, 1990)

¹¹ S.-R. Eric Yang and A. H. MacDonald, *Phys. Rev. B* **66**, 041304(R) (2002)

¹² C. de C. Chamon and X. G. Wen, *Phys. Rev. B*, **49** 8227 (1994)

¹³ S.M. Reimann, M. Koskinen, M. Manninen, and B.R. Mottelson *Phys. Rev. Lett.* **83**, 3270(1999)

¹⁴ C.J. Pethick, and H. Smith, *Bose-Einstein condensation in dilute gases*. (Cambridge University Press, Cambridge, 2002)

¹⁵ B. Mottelson, *Phys. Rev. Lett.* **83**, 2695 (1999)

¹⁶ N. R. Cooper, N. K. Wilkin and J. M. F. Gunn, *Phys. Rev. Lett.* **87**, 120405 (2001)

¹⁷ The word “yrast” originates from Swedish language and means “the most dizzy”

¹⁸ H. Saarikoski, S.M. Reimann, E. Räsänen, A. Harju, and M.J. Puska, accepted for publication in *Phys. Rev. B* (2005), cond-mat/0408448

¹⁹ M. Manninen, S. M. Reimann, M. Koskinen, Y. Yu and M. Toreblad, cond-mat/0410622